MORPHODYNAMIC MODEL TO SIMULATE SHORELINE EVOLUTION AT ANY COASTAL MOUND

Giuseppe R. Tomasicchio[1], Antonio Francone[2], Felice D'Alessandro[1], Gabriela Medellín[3], Alec Torres-Freyermuth[3], Giuseppe Barbaro[4] and Ferdinando Frega[2]

The work presents the results of a field and numerical study aimed to investigate the resistance and resilience, associated to an artificial shoreline perturbation, on a sandy beach. A temporary groin was deployed on a micro-tidal sea-breeze dominated beach to induce a shoreline perturbation. Wave conditions during the field experiment were highly correlated with sea breeze wind events, inducing a persistent alongshore sediment transport. A new one-line numerical model of beach evolution was calibrated and verified with the field surveys, reproducing both the sediment impoundment and subsequent beach recovery after the groin removal. Thus, the numerical model was able to simulate the mechanisms controlling the growth and decay caused by an artificial perturbation.

Keywords: numerical model, shoreline evolution, coastal morphodynamics, longshore transport, sediment transport

INTRODUCTION

The beach resistance, in coastal engineering, can be related to the shoreline evolution produced by extreme events and/or the presence of coastal structures altering the pattern of sediment transport in coastal areas; thus, the beach resistance is a measure of the beach capability to resist deviations with respect to an equilibrium morphological condition. On the other hand, the beach resilience determines the speed with which the beach morphology returns to the pre-disturbed condition (Orwin and Wardle 2004). Therefore, the knowledge of the beach stability (resistance and resilience) is fundamental for decision-making regarding the removal of existing infrastructure (e.g., groins) or their replacement by hybrid solutions (Sutton et al. 2015) as a mitigation measure against beach erosion.

The beach erosion along the northern Yucatan coast is significant due to the presence of coastal structures (Lira-Pantoja et al. 2012; Medellín et al. 2015); for this reason, structure removal was considered as a mitigation measure against beach erosion in this region (Medellín et al. 2015). However, no information regarding the mechanisms controlling the recovery of the shoreline position after structure removal is available.

An accurate estimation of alongshore sediment transport is fundamental for the evaluation of the beach stability in presence of coastal structures; it can be well determined by the implementation of an impoundment technique based on the use of a temporary groin in a field-based study. This approach was applied on sand (Bodge and Dean 1987; Wang et al. 1999) and mixed beaches (Martín-Grandes et al. 2009). The beach morphology changes observed in previous studies were considered for the estimation of the K value in the CERC equation (Rosati et al. 2002). Wang et al. (1999) reported values of 0.04 to 0.54, whereas Martin-Grandes et al. (2009) calibrated a one-line model finding that K=0.06-0.10. Recent studies have focused on investigating the morphodynamic responses to seafloor artificial perturbations (e.g., excavated holes and channels) in the nearshore (Elgar et al. 2012; Moulton et al. 2014, Moulton et al. 2017). Moulton et al. (2014) investigated the mechanisms controlling the infill of large excavated holes in the surf zone, finding that downslope gravity-driven bedload transport was important in morphological evolution for bathymetric features with large slopes. However, studies incorporating resilience for coastal engineering applications are scarce (Tomasicchio et al. 2011; D'Alessandro et al. 2012, D'Alessandro et al. 2016; Smith et al. 2017) and no-previous studies were devoted to investigate the beach recovery associated to structures removal. Thus, in order to address this, a field and numerical study was conducted on sandy beaches.

The present work aims to investigate the shoreline resistance and resilience on a sea-breeze dominated beach by means of field observations and numerical modelling. A temporary groin was deployed on a barrier island in the northern Yucatan Peninsula to induce a shoreline perturbation. A new one-line numerical model was calibrated and verified with the field surveys. The model was able to evaluate the capabilities to reproduce both the sediment impoundment and subsequent beach recovery after the groin removal.

[1] Department of Engineering, University of Salento, Lecce, 73100, Italy
[2] Department of Engineering, University of Calabria, Arcavacata di Rende, 87036, Italy
[3] Instituto de Ingeniería, Universidad Nacional Autónoma de México, Sisal, Yucatán, 97835, México
[4] Department of Engineering, Mediterranea University of Reggio Calabria, Reggio Calabria, 89100, Italy

FIELD EXPERIMENT

The field experiment has been conducted in Spring, 2015 at Sisal beach. A temporary groin has been deployed on morning (08:00) of May 27th to investigate the beach resistance. Moreover, the groin has been removed 24-hours later on the morning of May 28th and beach surveys continued for the following days until beach recovery, to investigate the beach resilience.

Study area

The study area is located on a barrier island in the northern Yucatan Peninsula (Figure 1a), at the fishing village of Sisal, 40 km west of the commercial port of Progreso. The area is characterized by a micro-tidal range, intense sea breeze conditions, and low energy waves. The field experiment site has been located between the Sisal Port and the Sisal Pier (Figure 1b). Moreover, winds, offshore waves, and mean sea level have been observed by UNAM (Universidad Nacional Autónoma de México) over the past years in order to characterize the main forcing mechanisms affecting the coastal region.

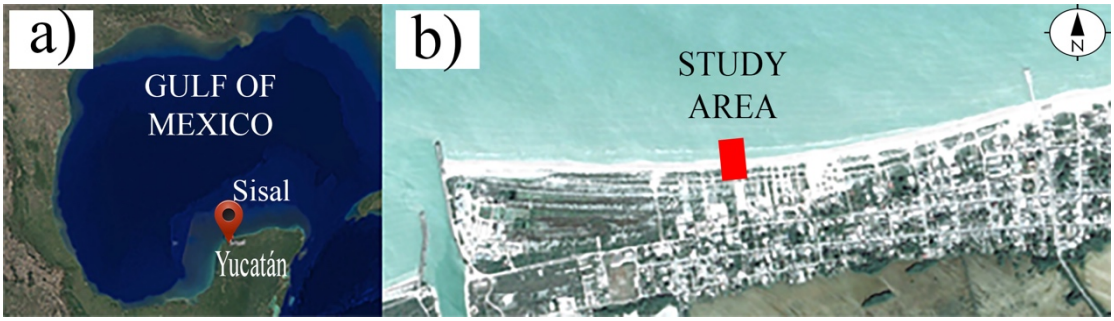

Figure 1. Location map showing (a) the Yucatan peninsula at the SE of the Gulf of Mexico, (b) the study area

Beach morphology

A bathymetric survey of the study area shows the presence of a sand bar system (Figure 2). The outer bar is relatively uniform alongshore, whereas inner bars present a high seasonal variability at some location. However, the beach orientation between the Sisal port and Sisal pier is relatively uniform for a 1 km stretch of coast located in the middle section. Beach evolution during the intense sea breeze season (May-September), at the two transects bounding the study area and represented in Figure 2, presented low variability (±3 m) in the shoreline position. Therefore, a temporary groin has been deployed between these two transects, owing to the low natural beach variability observed at this location, in order to assess beach resistance.

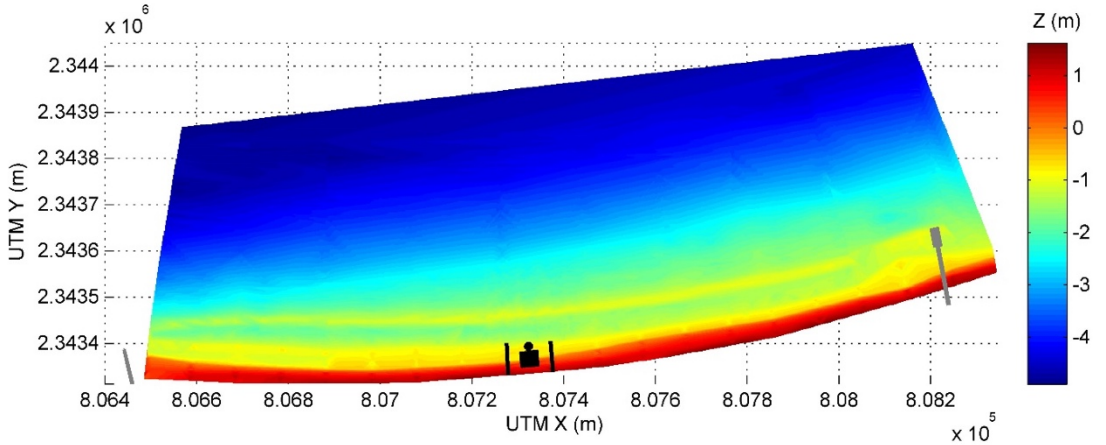

Figure 2. Bathymetry observed two days before the experiment (05/25/2015), showing the study area (■), the ADV (●), and the updrift/downdrift control lines (black solid lines) locations. The study site is located between the jetty of the Sisal port entrance channel (left-hand side, gray line) and the Sisal pier (right-hand side gray feature).

Wind and wave conditions

Wind velocity time series show a diurnal cycle associated with sea breeze events (Figure 3a). A maximum wind speed of 16 ms^{-1}, corresponding to an intense sea breeze event, has been recorded in the afternoon (16:30 local time) of May 27th (Figure 3a). The wave height increased from H_s = 0.3 m measured at 10:00 to H_s = 1.0 m measured at 18:00 (Figure 3b). The temporary structure was deployed during neap tide (Figure 3c) in order to decrease the influence of the tide on the effective length of the groin and hence restricting the swash zone width (e.g., Wang and Kraus 1999).

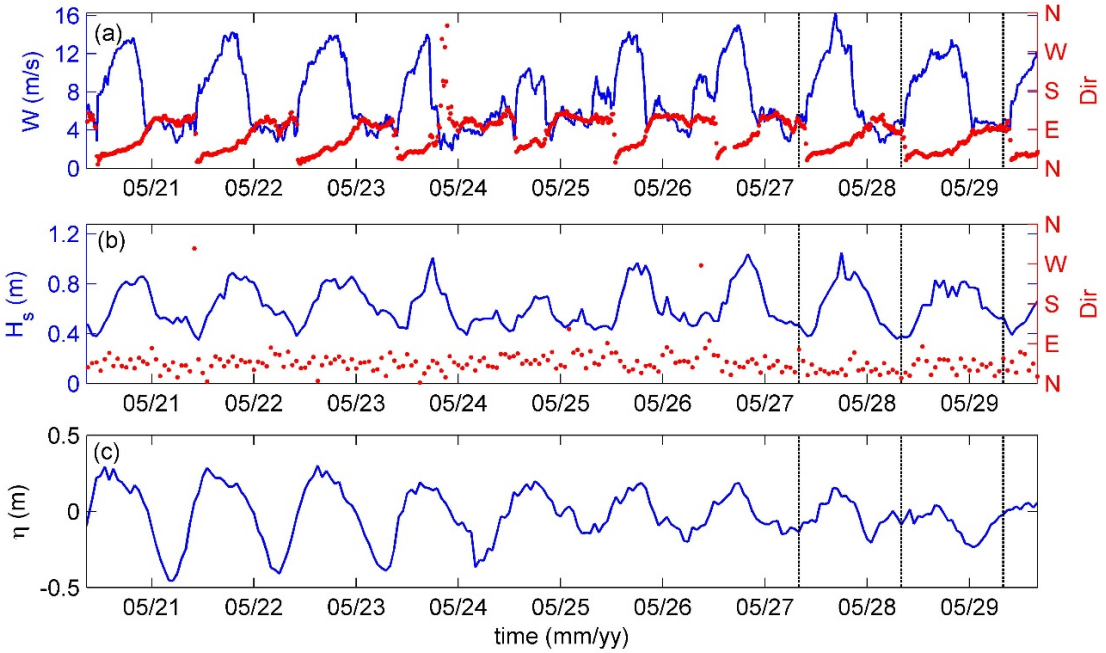

Figure 3. Measured (a) wind speed and wind direction (b) offshore significant wave height and wave direction at 10 m water depth, and (c) sea level from Sisal tide gauge before, during, and after the experiment. Vertical dashed lines indicate the boundaries of groin/no groin period.

Offshore wave conditions, observed at 10 m water depth using an RDI Acoustic Doppler Current Profiler (ADCP) located 11 km offshore, are characterized by NE waves highly correlated with local winds (Figure 4).

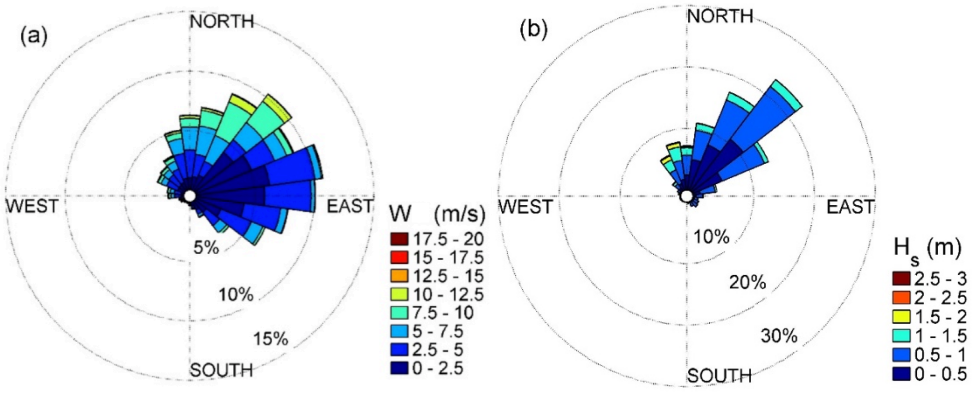

Figure 4. (a) Wind and (b) wave roses in the study area. Wind data are taken from the Sisal weather station MeteoSisal (www.weather underground.com 01/01/2009-06/17/2016) and the wave data have been collected from an ADCP located at 10 m water depth in front of Sisal (12/10/2013-4/20/2016).

Temporary groin

The temporary groin built for the present study has been based on the design proposed by Wang and Kraus (1999) for similar field conditions. Wood-sections 0.19 m thick of 2.40 m by 1.20 m have been deployed using a frame made of iron pipes and clamps (Figure 5). Holes (8 cm diameter) have been drilled and covered with a 63 m sieve cloth in order to avoid a returning offshore flow near the structure (Wang and Kraus 1999). The groin consisted of six and a half sections, with a 20 cm overlap between sections, resulting on a total length of 14.4 m. Furthermore, sandbags have been deployed along the base of the structure to avoid bed scouring that leaded to the sediment bypass.

Figure 5. Temporary groin

Beach morphology changes

Beach morphology changes have been investigated by analyzing the high-temporal resolution RTK-DGPS (Real Time Kinematic Global Positioning System) survey data observed at 15 survey lines covering the up-drift and down-drift sides of the temporary groin. The beach surveys have been conducted every two hours for 24-hours to evaluate the impact of the groin on the beach morphology. Furthermore, measurements continued after the groin removal with the same temporal resolution for 10 hours and they have been continued with a lower temporal resolution (from May 29th to June 3rd) to evaluate the complete beach recovery.

The observed beach survey before the groin deployment (07:30 of the 27/05/2015) presents an alongshore uniformity of the beach (Figure 6a). The deployment of a temporary impermeable structure (at x = 0 m) induces, after 24 hours a sediment impoundment at the up-drift side (east) of the structure and erosion at the down-drift side (west), consistent with the westward alongshore sediment transport associated to the sea breeze events (Figure 6b). The maximum shoreline advance, at the up-drift side of the groin, has been about 6 m; the shoreline retreat, at the down-drift side of the groin, has been less than 4 m. On the other hand, 24 hours after the structure removal (08:25 of the 29/05/2015) the beach morphology presented alongshore uniformity for the submerged area ($h < 0$ m), but a clear disturbance in the subaerial beach (Figure 6c). The disturbance smoothed out during the following days and became negligible 1 week after the structure removal on the 03/06/2015 (Figure 6d).

The calculated sediment volume impoundment, at the up-drift side of the groin, reached 70 m^3 in 24 hours, whereas the volume loss at the down-drift for the same period was less than 40 m^3. Differences between up-drift and down-drift volume changes might be attributed to the limited alongshore spatial coverage of the topographic measurements.

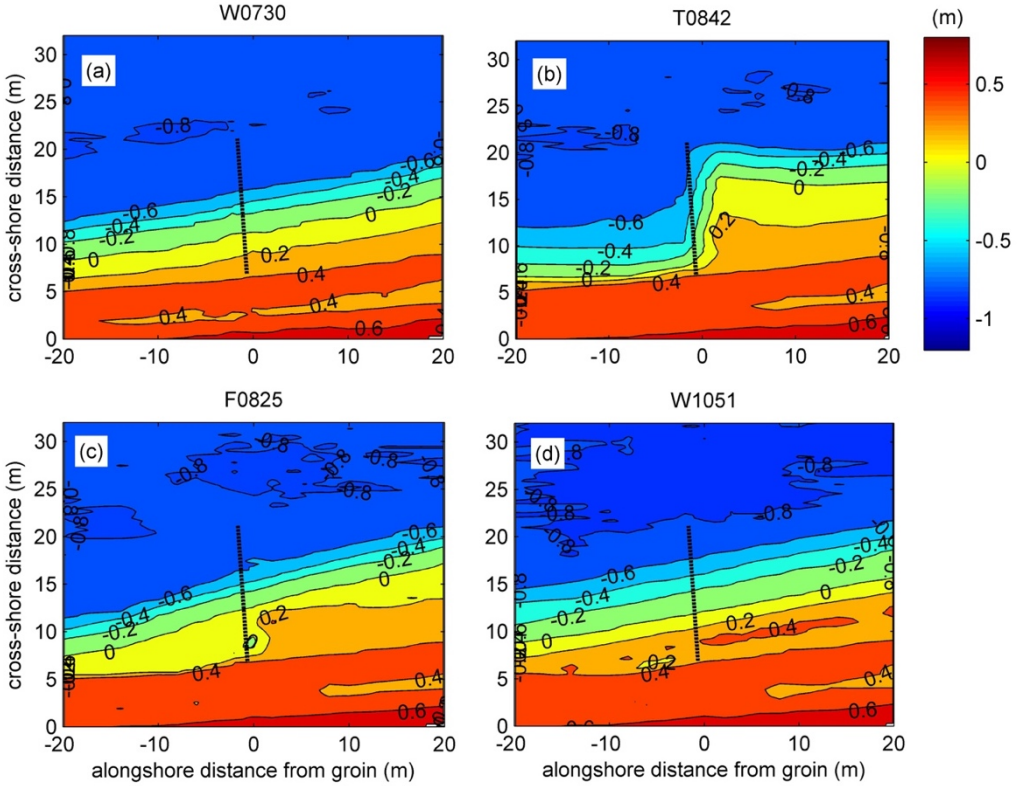

Figure 6. Beach survey(a) before groin deployment, (b) before groin removal, (c) 24 hours after groin removal, (d) 144 hours after groin removal

NUMERICAL MODELLING

Model description

Numerical simulations have been conducted by means of a newly proposed morphodynamic model, named General Shoreline beach 1.0 (GSb), belonging to the one-line model typology (Frey et al. 2012). This typology assumes that the beach cross-shore profile remains unchanged (Bruun 1954; Dean 1990), thereby allowing beach change to be described uniquely in terms of the shoreline position. The peculiarity of the GSb model consists of simulating shoreline evolution based on a longshore transport formula/procedure suitable at any coastal mound: sand, gravel, cobbles, shingle and rock beaches (Tomasicchio et al. 1994; Lamberti and Tomasicchio 1997; Tomasicchio et al. 2007; Tomasicchio et al. 2013; Tomasicchio et al. 2015; Tomasicchio et al. 2016). The GSb model presents one calibration coefficient solely, K_{GSB}, which does not depend on the grain size diameter and depends on the alongshore gradient in breaking wave height (Ozasa and Brampton 1980). As a consequence, differently from other morphodynamics models, GSb calibration is not based on the comparison of historical observed shorelines. The proposed general formula/procedure considers an energy flux approach combined with an empirical/statistical relationship between the wave-induced forcing and the number of moving units. GSb model allows to determine short-term (daily base) or long-term (years base) shoreline change for arbitrary combinations and configurations of structures (groins, jetties, detached breakwaters, and seawalls) and beach fills that can be represented on a modelled reach of coast.

GSb simulations

Field conditions have been adopted to perform numerical simulations by GSb. Thus, a 14.4 m long groin (10 m wet plus 4.4 m dry) has been positioned at the center of the domain. The alongshore computational domain has been assumed equal to 41 m. Model grid cell resolution, DX, has been set equal to 1 m with a total number of cells, NX, equal to 41, whereas the model experiment has been simulated adopting a calculation time step, DT, equal to 0.005 hours. For a direct comparison with field

measurements, the recording time step of the output files has been set to 1 hour The median grain size, D_{50}, has been set to 0.3 mm as measured at this field site (Wellman 2014) and the depth of closure has been considered equal to d_c = 0.8 m. The hourly wave conditions recorded at the ADCP located 11 km offshore the beach have been adopted as input to the GSb model.

A sensitivity analysis of K_{GSB} parameter has been conducted in order to calibrate the model with the observed field data (Figure 7).

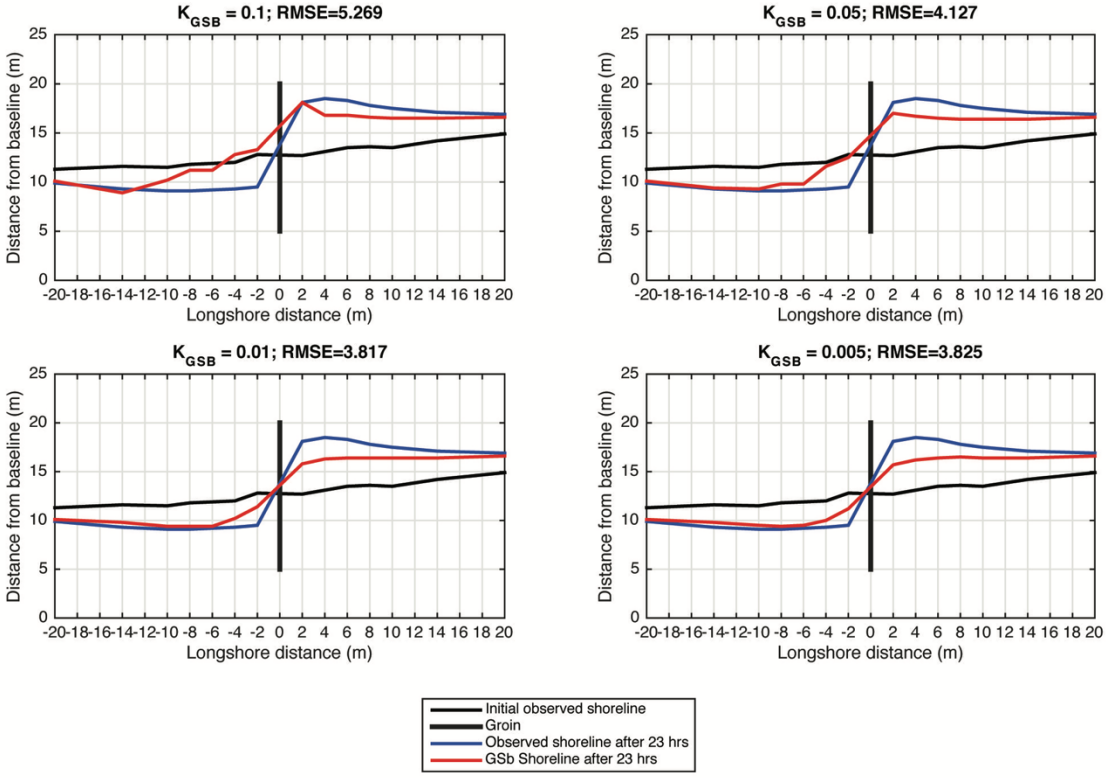

Figure 7. Sensitivity analysis of K_{GSB} parameter

The root mean square error has been calculated (Table 1) in order to compare, for different K_{GSb} values, the observed and calculated shoreline positions at 23 hours after the groin deployment; the RMSE is defined as,

$$RMSE = \sqrt{\frac{\sum_{i=1}^{N}\left(y_{i,GSb}-y_{i,obs}\right)^2}{N}} \qquad (1)$$

where N is the number of transects considered in the computational domain.

Table 1. Observed and calculated shoreline positions at 14 transects along the shoreline and relative values of RMSE (Root Mean Square Error)

Longshore distance from groin (m)		*-20*	*-14*	*-10*	*-8*	*-6*	*-4*	*-2*	*2*	*4*	*6*	*8*	*10*	*14*	*20*	*RMSE*
Distance from baseline (m)	*Obs. Initial Shoreline*	11.3	11.6	11.5	11.8	11.9	12.0	12.8	12.7	13.1	13.5	13.6	13.5	14.2	14.9	
	Obs. Final Shoreline	9.9	9.3	9.1	9.1	9.2	9.3	9.5	18.1	18.5	18.3	17.8	17.5	17.1	16.9	
	Calc. - K_{GSB}=0.005	10.1	9.8	9.5	9.4	9.5	10.0	11.2	15.7	16.2	16.4	16.5	16.4	16.4	16.6	3.825
	Calc. - K_{GSB} = 0.01	**10.1**	**9.8**	**9.4**	**9.4**	**9.4**	**10.2**	**11.4**	**15.8**	**16.3**	**16.4**	**16.4**	**16.4**	**16.4**	**16.6**	**3.817**
	Calc. - K_{GSB} = 0.05	10.1	9.4	9.3	9.8	9.8	11.6	12.5	17.0	16.7	16.5	16.4	16.4	16.4	16.6	4.127
	Calc. - K_{GSB} = 0.1	10.1	8.9	10.2	11.2	11.2	12.8	13.3	18.1	16.8	16.8	16.6	16.5	16.5	16.6	5.269

A K_{GSb} = 0.01 value has determined a better agreement between the observed and the calculated shoreline positions.

The first beach survey has been assumed as the initial shoreline position in the numerical model. GSb lateral boundaries have been selected as moving boundaries. If a moving lateral boundary condition is selected, the boundary will move a specified distance over a certain time period. In particular, at the down-

drift (x = -20 m) and up-drift (x = +20 m) boundaries of the computational domain, the observed specific distances from the first beach survey, equal to -1.4 m and 1.8 m, respectively, over a period of 24 hours, have been assumed. On the other hand, for the post groin removal condition the computation duration has been extended to 168 hours.

Figures 8c-h show that the calibrated numerical model satisfactorily predicts the down-drift shoreline evolution, whereas the maximum shoreline advance, at t = 21 hours, in the up-drift side is under-predicted (Figure 8h).

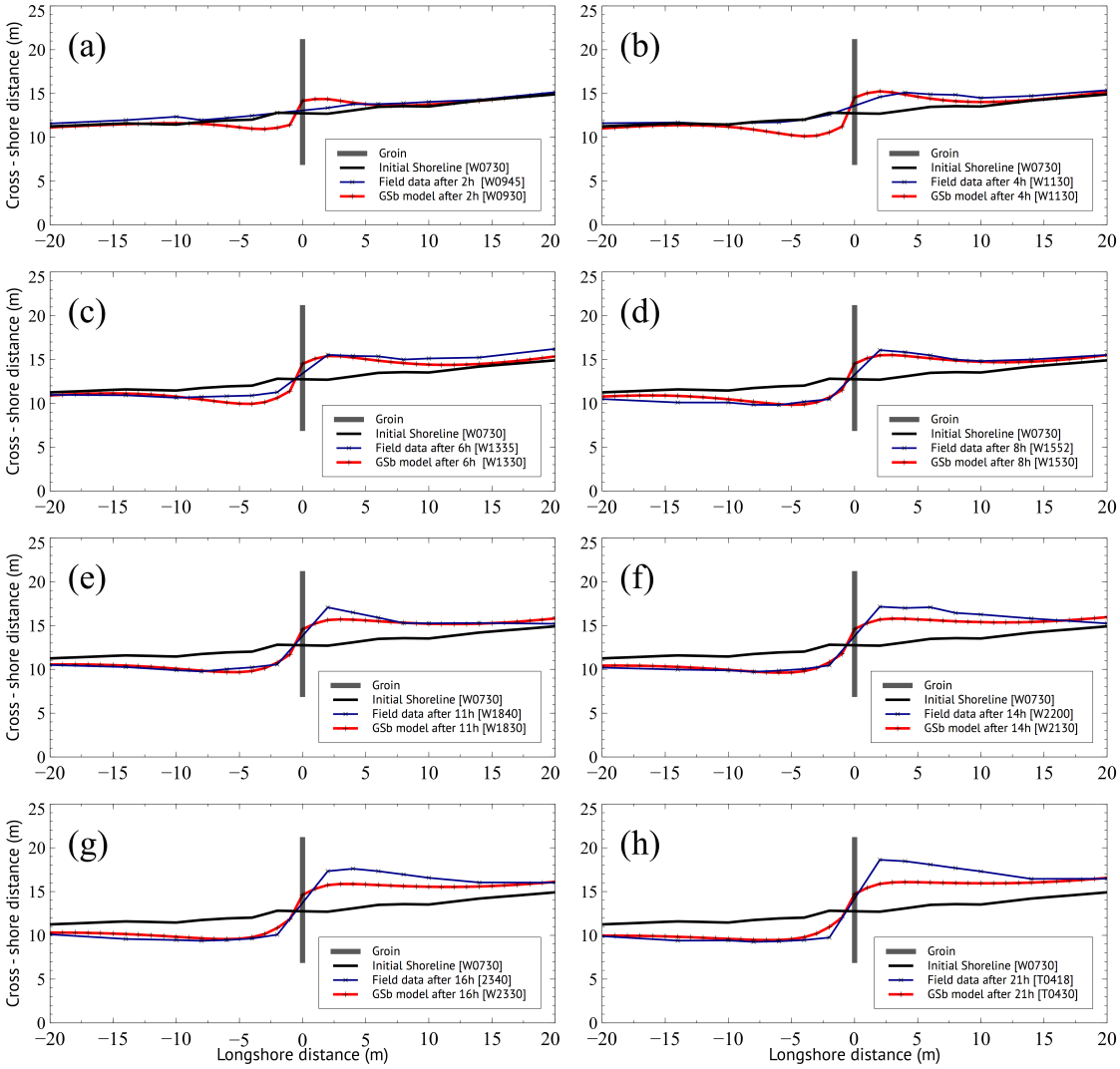

Figure 8. Observed and calculated shoreline position (a) 2 h, (b) 3 h, (c) 6 h, (d) 7 h, (e) 11 h, (f) 14 h, (g) 16 h, (h) 21 h after the groin deployment.

The GSb model capability to calculate the beach behavior after the groin removal (resilience) has been investigated. The beach position immediately before the groin removal has been assumed as initial shoreline position and the numerical model was run without the impermeable groin using the daily mean conditions as observed for the following seven days. The numerical model predicted the drastic change occurring during the first 24 hours after the groin removal (Figures 9a-e). Furthermore, it has been able to predict the beach recovery occurring after approximately 1 week (Figure 9f). Therefore, within the framework of the field data gained in the investigation (sea-breeze conditions), the model can be considered as a reliable tool to conduct a numerical study on beach resistance and resilience for the adopted study area.

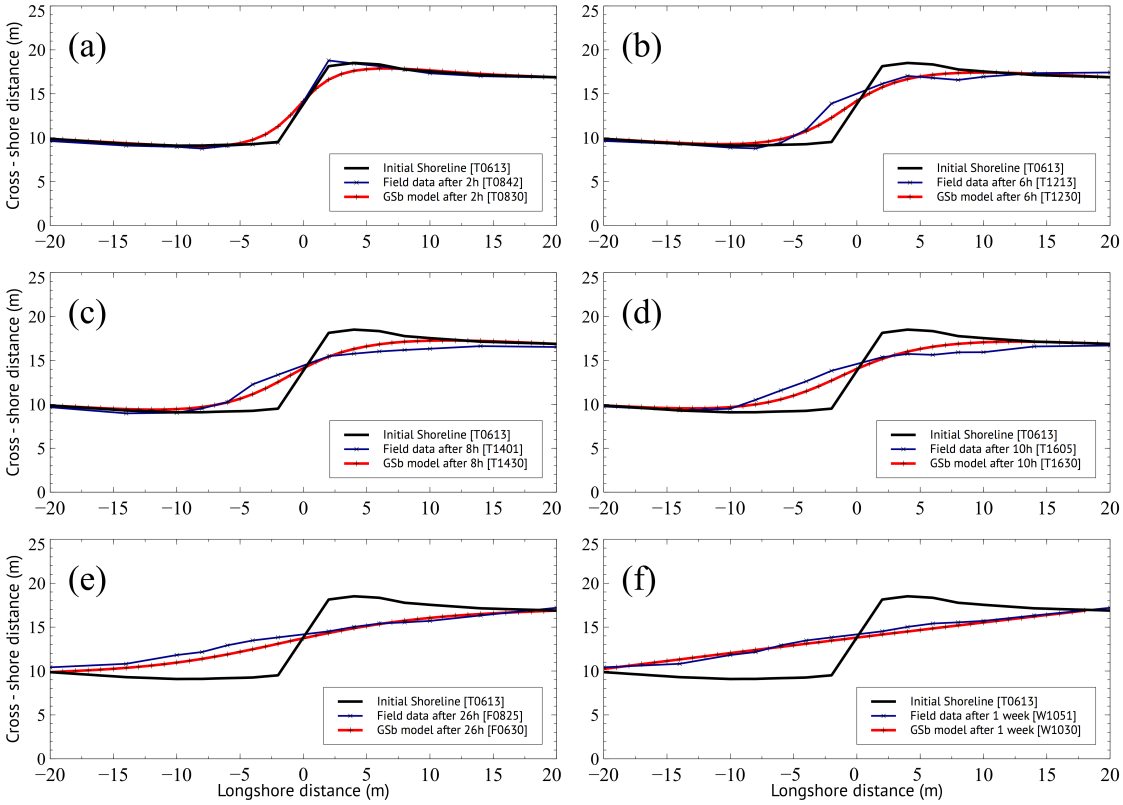

Figure 9. Observed and calculated shoreline position (a) 2 h, (b) 6 h, (c) 8 h, (d) 10 h, (e)26 h and (f) 1 week after the groin removal.

CONCLUSIONS

A field and numerical study of shoreline resistance and resilience was conducted on a sea breeze dominated sandy beach. The field study consisted on the deployment of a temporary impermeable groin to induce a shoreline perturbation in the swash zone. Furthermore, impermeable groin removal 24 hours after deployment allowed us to study the shoreline recovery. Analysis of high-spatial resolution field observations showed significant beach morphology changes owing to the structure and the evolution toward the initial state in the following days after the structure removal. A new shoreline evolution numerical model, General Shoreline beach (GSb), was employed to investigate the resistance and resilience shoreline evolution. The value of the adopted calibration coefficient in the GSb model was found by comparing the observed and calculated shorelines at the end of the groin presence (23 hours) by means of a sensitivity analysis of K_{GSB} value. The calibrated model was verified by simulating the shoreline and comparing it with the observed one; the comparison resulted favorable. Therefore, GSb model can be considered as a reliable tool to conduct a numerical study on beach resistance and resilience limited to the prevailing wave conditions (sea-breeze generated) for the adopted study area. Further possible research might be conducted, comparing the GSb model results against resistance and resilience data from not sandy beaches, with the possibility to include the influence of tidal variation on calculated shoreline position.

ACKNOWLEDGMENTS

We acknowledge the field support provided by students and researchers at the Laboratorio de Ingeniería y Procesos Costeros at UNAM, especially from Gonzalo Uriel Martín Ruiz, David A. Gracia, Elena Ojeda, Tonatiuh Mendoza, José Carlos Pintado-Patiño, José Alberto Zamora, Daniel Toxtega, Martín Ezquivelzeta, Miguel Ángel Valencia, Paola Espadas, Luis Ángel Gallegos, Daniel Pastrana, Jesús Aragón, Pedro Cabañas, Alejandro Astorga, Enna López, Rafael Meza, Wilmer Rey, and Marcos García.

The present research was funded by the Apulia Region (Italy), through the Regional Cluster Project "Eco-Smart Breakwater", Grant # C6LU5I7.

REFERENCES

Bodge, K. R., and R.G. Dean. 1987. Short-Term Impoundment of Longshore Sediment Transport, TR CERC-87-7, *WES*, Vicksburg, Miss.

Bruun, P. 1954. Coast erosion and the development of beach profiles, *Technical Memorandum N. 44*, Beach Erosion Board.

D'Alessandro, F., G.R. Tomasicchio, F. Musci, and A. Ricca. 2012. Dune erosion physical, analytical and numerical modelling, *Proceedings 33rd International Conference on Coastal Engineering*, Santander, printed on-line, paper n. sediment.32.

D'Alessandro, F., and G.R. Tomasicchio. 2016. Wave-dune interaction and beach resilience in large-scale physical model tests, *Coastal Engineering*, 116, 15–25.

Dean, R.G. 1990. Equilibrium beach profiles: characteristics and applications, *Journal of Coastal Research*, 71(1), 53-84.

Elgar, S., B. Raubenheimer, J. Thomson, and M. Moulton. 2012. Resonance in an evolving hole in the swash zone, *J. Waterway, Port, Coastal, Ocean Eng.*, 138, No. 4, 299-302.

Folke, C. 2006. Resilience: The emergence of a perspective for social-ecological systems analyses, *Global Environmental Change*, 16, pp. 253-267.

Frey, A.E., K.J. Connell, H. Hanson, M. Larson, R.C. Thomas, S. Munger, and A. Zundel. 2012. GenCade Version 1 Model Theory and User's Guide, *Tech. Report ERDC/CHL TR-12-25*, U.S. Army Engineer Res. and Development Center, Vicksburg, MS.

Lamberti, A., and G.R. Tomasicchio. 1997. Stone mobility and longshore transport at reshaping breakwaters, *Coastal Engineering*, 29, 263-289.

Lira-Pantoja, M., A. Torres-Freyermuth, C. Appendini, D. Fernández, P. Salles, E. Mendoza, J. López, and A. Pedrozo-Acuña. 2012. Chronic beach erosion induced by coastal structures in Chelem, Yucatan, *Proceedings of the 33rd International Conference,* Santander, Spain, ISSN: 2156-1028.

Martin-Grandes, I., J. Hughes, D. J. Simmonds, A. J. Chadwick, and D. E. Reeve. 2009. Novel methodology for one line model calibration using impoundment on mixed beach, *Coastal Dynamics 2009 - Impacts of Human Activities on Dynamic Coastal Processes*.

Masselink, G., B. Castelle, T. Scott, G. Dodet, S. Suanez, D. Jackson, and F. Floc'h. 2016. Extreme wave activity during 2013/2014 winter and morphological impacts along the Atlantic coast of Europe, *Geophys. Res. Lett.*, 43, 2135–2143.

Medellín, G., I. Mariño-Tapia, and J. Euán-Ávila. 2015. The influence of a seawall on postnourishment evolution in a sea-breeze-dominated microtidal beach, *Journal of Coastal Research*, 31(6), 1449–1458. Coconut Creek (Florida), ISSN 0749-0208.

Moulton, M., S. Elgar, and B. Raubenheimer. 2014. A surf zone morphological diffusivity estimated from the evolution of excavated holes, *Geophys. Res. Lett.*, 41, 4628-4636.

Moulton, M., S. Elgar, B. Raubenheimer, J.C. Warner, and N. Kumar. 2017. Rip currents and alongshore flows in single channels dredged in the surf zone, *J. Geophys. Res. Oceans*, 122, 3799-3816.

Orwin, K. H., and D. A. Wardle. 2004. New indices for quantifying the resistance and resilience of soil biota to exogenous disturbances, *Soil Biology & Biochemistry*, 36: 1907-1912.

Ozasa, H., and A.H. Brampton. 1980. Mathematical modeling of beaches backed by seawalls, *Coastal Engineering*, 4, 47-64.

Pimm, S. L. 1984. The complexity and the stability of ecosystems, *Nature*, 307, 321-326.

Rosati, J. D., T. L. Walton, and K. Bodge. 2002. Longshore sediment transport, in Coastal Engineering Manual, part III, edited by D. B. King, *Tech. Rep. EM 1110-2-1100*, U. S. Army Corps of Eng., Washington, D. C.

Smith, E.R., F. D'Alessandro, G.R. Tomasicchio, and J.Z. Gailani. 2017. Nearshore placement of a sand dredged mound*, Coast. Eng.*, 126, 1–10.

Sutton-Grier, A. E., K. Wowk, and H. Bamford. 2015. Future of our coasts: The potential for natural and hybrid infrastructure to enhance the resilience of our coastal communities, economies and ecosystems, *Environmental Science & Policy*, 51, 137-148.

Tomasicchio, G.R., A. Lamberti, and F. Guiducci. 1994. Stone movement on a reshaped profile, *Proceedings of the 24th International Conference on Coastal Engineering*, 2, 1625–1640.

Tomasicchio, G.R., R. Archetti, F. D'Alessandro, and P. Sloth. 2007. Long-shore transport at berm breakwaters and gravel beaches, *Proceedings International Conference Coastal Structures '07*, Venice, 65-76.

Tomasicchio, G.R.; A. Sanchez Arcilla, F. D'Alessandro, S, Ilic, M. James, C.J.E.M. Fortes, F. Sancho, and H. Schüttrumpf. 2011. Large-scale flume experiments on dune erosion processes, *J. Hydraul. Res.*, 49, 20–30.

Tomasicchio, G.R., F. D'Alessandro, G. Barbaro, and G. Malara. 2013. General longshore transport model, *Coastal Engineering*, 71, 28-36.

Tomasicchio, G.R., F. D'Alessandro, G. Barbaro, E. Musci, and T.M. De Giosa. 2015. Longshore transport at shingle beaches: an independent verification of the general model, *Coastal Engineering*, 104, 69-75.

Tomasicchio, G.R., F. D'Alessandro, G. Barbaro, A. Francone, and S.M. Kurdistani. 2016. General model for estimation of longshore transport at shingle/mixed beaches, *Proceedings 35th International Conference on Coastal Engineering*, Antalya.

Wang, P., and N. C. Kraus. 1999. Longshore sediment transport rate measured by short-term impoundment, *Journal of Waterway, Port, Coastal, and Ocean Engineering*, Vol. 125, No. 3, pp. 118-126.

Wellmann, N. 2014. Analysis of near-shore sediment samples from Sisal Beach (Mexico) comparing effects of sea breeze and el Norte events, *MSc, Thesis*, Hochschule für Technik, Wirtschaft und Kultur Leipzig.

Van Rijn, R., and W. Van Der Werf. 2013. Coastal sediment dynamics: recent advances and future research needs, *Journal of Hydraulic Res.*, 51:5, 475-493.